ISSN (Print) 1226-1750
ISSN (Online) 2233-6656
Journal of Magnetics 28(1), 24-33 (2023) https://doi.org/10.4283/JMAG.2023.28.1.024

Thermal Conductivity and Mixed Convection Influence on the Flow of Viscoelastic Fluid Due To Inclined Cylinder

Tasawar Abbas[1]*, Munazza Saeed[1], Kaouther Ghachem[2], Badr M. Alshammari[3], Sami Ullah Khan[4], and Lioua Kolsi[5,6]

[1]Department of Mathematics, University of Wah, Wah Cantt, 47040 Pakistan
[2]Department of Industrial Engineering and Systems, College of Engineering, Princess Nourah bint Abdulrahman University, P.O. Box 84428, Riyadh 11671, Saudi Arabia
[3]Department of Electrical Engineering, College of Engineering, University of Ha'il, Ha'il City, Saudi Arabia
[4]Department of Mathematics, Namal University, Mianwali 42250, Pakistan
[5]Department of Mechanical Engineering, College of Engineering, University of Ha'il, Ha'il City, Saudi Arabia
[6]Laboratory of Metrology and Energy Systems, National Engineering School, Energy Engineering Department, University of Monastir, 5000 Monastir, Tunisia

(Received 6 October 2021, Received in final form 10 January 2023, Accepted 16 March 2023)

The thermal flow of second grade fluid with Soret and Dufour effects has been observed in this investigation. The problem is modified with mixed convection and thermal radiation applications. The thermal conductivity with variable relations is used to analyze the transport phenomenon. Further, the applications of mixed convection and magnetic force has also been focused. The convective thermal and concentration flow constraints are used for the current flow problem. The shooting numerical scheme is used to calculate the numerical observations. The major impact of parameters is visualized for flow parameters. It is observed that the velocity profile increases for curvature parameter and viscoelastic fluid parameter. The assumptions of variable thermal conductivity enhanced with transport phenomenon. The Nusselt number declined for variable thermal conductivity parameter.

Keywords : second grade fluid, variable thermal conductivity, mixed convection flow, stretched cylinder, numerical scheme

1. Introduction

The phenomenon of heat and mass transfer is important from industrial and engineering point out view. The significant applications of transmission of heat as well as mass transport phenomenon is observed in cooling systems, heat transfer devices, spinning of fibers, chemical processes, food industry, petroleum sciences etc. In power industry, the combined heat and mass transfer phenomenon present novel applications. Different investigations are reported for heat and mass transfer phenomenon for linear and nonlinear fluid models. For instance, Hashim *et al.* [1] presented the mass and heat transfer aspect of Williamson fluid with unsteady flow. Bigdeli *et al.* [2] observed the combined thermal assessment of nanofluid with automotive applications. Tassaddiq *et al.* [3] investigated the rotating surface flow with combined transport via moving disk. Ahmed *et al.* [4] observed the circular motion of nanofluid for passage flow under improved heat transfer rate. Minaeian *et al.* [5] detected the physical implications of viscoelastic fluid with heat and mass pattern due to role of inertia regime. The thermos-diffusion applications with heat and mass transfer observations regarding the Williamson fluid was analyzed by Zhu *et al.* [6]. Shamshuddin *et al.* [7] reported the Hall impact conveying the power law velocity under thermal transport. The fractional computations for thermal problem owing to the slip boundary constraints was reflected by Raza *et al.* [8]. Ahmad *et al.* [9] reported the 3-D flow for Maxwell model under forced convection phenomenon. Abbasi *et al.* [10] analyzed the peristalsis evaluation of mass and heating phenomenon with Ellis fluid in channel. Saritha *et al.* [12] observed the ferromagnetic flow of

*Corresponding author: Tel: +92-51-9157000
e-mail: tasawar.abbas@uow.edu.pk

Sisko fluid with assessment of transport properties. Hayat *et al.* [13] reported the inclined surface flow with mechanism of heat and mass transport. Nazeer *et al.* [14] explained the onset of heat transfer for optimized flow due to Riga surface with Eyring Powell nanofluid. Khan *et al.* [15] addressed the aspect of Lorentz force due to paraboloid type of moving surface with Ree-Eyring nanofluid with imprved heat transfer phenomenon. Song *et al.* [16] examined the thermal diffusion aspect of heat transfer with Marangoni applications additionally impacted with radiative source. Khan *et al.* [17] reported the electromagnetic aspect of slip flow with nanomaterial via theoretical outcomes. The peristalsis flow of carbon nanotubes with entropy generation framework was concluded by Farooq *et al.* [18]. Zhao *et al.* [19] discussed the artificial neural network (ANN) analysis for heat transfer problem conveying the rotating disk.

In many heat and mass transfer problems, the fluctuation in heat transfer is resulted from two factors namely temperature gradient and concentration gradient. In thermal diffusion, the role of diffusion flux due to temperature gradient is important. This phenomenon is known as Soret effects. The reciprocal of Soret impact is know as Dufour impact which is association to the heat flux against chemical potential gradient. Different applications are conveyed in chemical processes and thermal engineering system. Some studies on thermos-diffusion phenomenon are presented in refs. [20-23].

Current research presents the thermos-diffusion flow of second grade fluid due to porous stretched cylinder. The problem is supported with following flow features:

- The heat and mass transport phenomenon for second grade fluid with Soret and Dufour effects is observed due to porous stretched cylinder.
- The analysis is supported with novel features of thermal radiation, viscous dissipation and magnetic force.
- The variable thermal conductivity observations are used to investigates the problem.
- The convective boundary constraints are used to identify the heat and mass transport rate.
- The numerical computation of problem is performed by using convective thermal and concentration boundary conditions.
- The physical impact of parameters due to flow parameters is observed.

It is remarked that different studies regarding the stretched cylinder flow are performed by researchers. However, the thermal-diffusion assessment of second grade fluid with variable thermal conductivity, viscous dissipation and radiative thermal phenomenon is not claimed yet. This model aims to fulfill this research gap. The applications are problem is presented for different flow parameters.

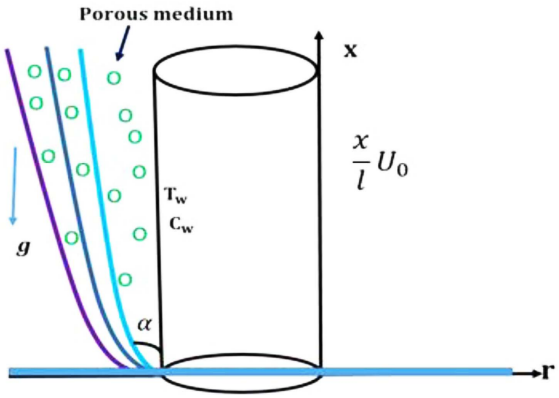

Fig. 1. (Color online) Geometry of the problem.

2. Problem Statement

The moving surface stretching flow due to cylinder with second grade fluid is presented (Fig. 1). The stretched cylinder moves with inclined direction having angle α. The mathematical modelling of problem is based on following flow assumptions:

i. A steady flow of second grade fluid with heat and mass transfer phenomenon is presented.
ii. The thermal-diffusion and viscous dissipation features are contributed in the heat equation.
iii. The viscosity of viscoelastic material is assumed to be variable.
iv. The thermal radiation impact is endorsed to observe the heat transfer phenomenon.
v. The source of flow is the stretched cylinder with porous medium saturation.
vi. The assessment of problem is claimed with convective boundary conditions.

The formulated problem with nonlinear partial differential equations is given as [22]:

$$\frac{\partial(ru)}{\partial x}+\frac{\partial(rv)}{\partial r}=0, \tag{1}$$

$$u\frac{\partial u}{\partial x}+v\frac{\partial u}{\partial r}=\nu\left(\frac{\partial^2 u}{\partial r^2}+\frac{1}{r}\frac{\partial u}{\partial r}\right)+g\beta(T-T_\infty)Cos(\alpha)+g\beta_c(C-C_\infty)Cos(\alpha)-\frac{\nu}{K}u+\frac{\alpha_1}{\rho}\left(v\frac{\partial^3 u}{\partial r^3}+u\frac{\partial^3 u}{\partial x\partial^2 r}+\frac{\partial u}{\partial x}\frac{\partial^2 u}{\partial r^2}-\frac{\partial u}{\partial r}\frac{\partial^2 v}{\partial r^2}+\frac{1}{r}\left(v\frac{\partial^2 u}{\partial r^2}+u\frac{\partial^2 u}{\partial r\partial x}+\frac{\partial u}{\partial r}\frac{\partial u}{\partial x}-\frac{\partial u}{\partial r}\frac{\partial v}{\partial r}\right)\right)-\frac{\sigma {B_0}^2}{\rho}u, \tag{2}$$

$$u\frac{\partial T}{\partial x}+v\frac{\partial T}{\partial r}=\frac{1}{\rho c_p}\frac{1}{r}\frac{\partial}{\partial r}\left(K(T)r\frac{\partial T}{\partial r}\right)+\frac{\mu}{\rho c_p}\left(\frac{\partial u}{\partial r}\right)^2-\frac{16\sigma^* T_\infty^3}{3k^*\rho c_p}\frac{\partial^2 T}{\partial r^2}+\frac{D_m k_T}{c_p c_s}\left(\frac{\partial^2 C}{\partial r^2}\right)+\frac{\alpha_1}{\rho c_p}\left(v\frac{\partial u}{\partial r}\frac{\partial^2 u}{\partial r^2}+u\frac{\partial u}{\partial r}\frac{\partial^2 u}{\partial x\partial r}\right)+\frac{\sigma {B_0}^2}{\rho c_p}u^2, \tag{3}$$

$$u\frac{\partial C}{\partial x}+v\frac{\partial C}{\partial r}=D_m\frac{1}{r}\frac{\partial}{\partial r}\left(r\frac{\partial C}{\partial r}\right)+\frac{V k_T}{T_m}\frac{1}{r}\frac{\partial}{\partial r}\left(r\frac{\partial T}{\partial r}\right). \tag{4}$$

with velocity components (u, v), gravity (g), inclined angle (α), material parameter (α_1), electric conductivity (σ), kinematic viscosity (ν), fluid density (ρ), permeability of porous space (K), temperature dependent thermal conductivity ($K(T)$) specific heat (c_p), fluid temperature (T) free stream temperature (T_∞) concentration (C) Stefan Boltzmann coefficient (σ^*) and mean absorption coefficient (k^*).

The boundary conditions are:

$$u(x)=u=\frac{U_o x}{L}, v=0, -k\frac{\partial T}{\partial r}=h(T_f-T),$$
$$-D_m\frac{\partial C}{\partial r}=k_m(C_f-C), at\ r=a$$
$$u\to 0,\ \frac{\partial u}{\partial r}\to 0,\ T\to T_\infty,\ C\to C_\infty,\ as\ r\to\infty. \tag{5}$$

with L (characteristics length) and reference velocity (U_o). The expressions satisfying the variable viscosity are:

$$K(T)=k_o(1+\in(T-T_\infty)). \tag{6}$$

with $\in$ (small distance) and k_o (coefficient of heat conductivity), k (thermal conductivity). The new variables are:

$$u=\frac{U_o x}{L}f'(\eta),\ v=-\sqrt{\left(\frac{\nu U_o}{L}\right)}f(\eta),\theta(\eta)=\frac{T-T_\infty}{T_f-T_\infty},$$
$$\phi(\eta)=\frac{C-C_\infty}{C_f-C_\infty},\eta=\frac{r^2-a^2}{2a}\sqrt{\frac{U_o}{\nu l}}, \tag{7}$$

The dimensionless system is:

$$(1+2\gamma\eta)f'''+2\gamma f''+ff''-f'^2-k_1 f'+4\gamma\beta(f'f''-ff''')+\beta(1+2\gamma\eta)(2f'f'''+f''^2-ff'''')-Ha^2 f'+Gr\theta Cos(\alpha)+Gc\phi Cos(\alpha)=0 \tag{8}$$

$$\left(1+\in\theta+\tfrac{4}{3}R\right)((1+2\gamma\eta)\theta'')+2\gamma\theta'\left(1+\tfrac{4}{3}R\right)+(1+2\gamma\eta)\theta'^2\in+Prf\theta'+Du\left((1+2\gamma\eta)\phi''+2\gamma\phi'\right)-PrEc\beta\gamma f f''^2+PrEc(1+2\gamma\eta)(f''^2-\beta f f''f'''+\beta f'f''^2)+PrEcHa^2 f'^2=0 \tag{9}$$

$$(1+2\gamma\eta)\phi''+2\gamma\phi'+Scf\phi'+Sr\left((1+2\gamma\eta)\theta''+2\gamma\theta'\right)=0 \tag{10}$$

satisfying:

$$f=0,\ f'=1,\ \theta'(0)=-B_{i1}(1-\theta(0)),\ \phi'(0)=-B_{i2}(1-\phi(0)),\qquad \eta=0$$
$$f'=0,\ f''=0,\ \theta=0,\ \phi=0,\qquad at\ \eta=\infty \tag{11}$$

where $\gamma=\sqrt{\frac{\nu L}{a^2 U_o}}$ is curvature parameter, $Gr=\frac{g\beta(T_f-T_\infty)l^2}{xU_o^2}$ is thermal Grashof number, $Gc=\frac{g\beta_c(C_f-C_\infty)l^2}{xU_o^2}$ is solutal Grashof number, $k1=\frac{\nu L}{KU_o}$ porosity parameter, $Pr=\frac{\nu}{k_o}$ Prandtl number, $Du=\frac{D_m k_T}{c_p c_s}\frac{\rho c_p}{k}\frac{C_f-C_\infty}{T_f-T_\infty}$ is Dufour number, $Sr=\frac{k_{T(T_f-T_\infty)}}{T_m(C_f-C_\infty)}$ Soret number, $Ec=\frac{U_O^2\left(\frac{x}{L}\right)^2}{c_p(T_f-T_\infty)}$ is Eckret number, $Sc=\frac{\nu}{D_m}$ is Schmidt number, $B_{i1}=\frac{h}{k}\sqrt{\frac{\nu L}{U_o}}$ is thermal Biot number, $R=\frac{4\sigma^* T_\infty^3}{k^* k_o}$ be radiation parameter, $\beta=\frac{\alpha_1 U_o}{\rho\nu L}$ is the viscoelastic parameter and $Ha=\frac{\sigma {B_0}^2 L}{\rho U_o}$ is Hartmann number.

The Nusselt number, Sherwood number and wall shear force is defined as:

$$Nu_x=\frac{xq_w}{k(T_f-T_\infty)},\ q_w=-k\frac{\partial T}{\partial r}-\frac{16\sigma T_\infty^3}{3k^*}\frac{\partial T}{\partial r}|_{r=a}, \tag{12}$$

$$Sh_x=\frac{J_w x}{D_m(C_f-C_\infty)},\ J_w=-D_m\frac{\partial C}{\partial r}|_{r=a}, \tag{13}$$

$$C_{fx}=\frac{2\tau_w}{\rho u_w^2},\ u_w=U_0\left(\frac{x}{l}\right)and\ \tau_w=\mu\frac{\partial u}{\partial r}|_{r=a}. \tag{14}$$

These quantities in dimensionless form are follows as:

$$\frac{Nu_x}{Re_x^{\frac{1}{2}}}=-\left(1+\in\theta+\frac{4}{3}R\right)\theta'(0), \tag{15}$$

$$\frac{Sh_x}{Re_x^{\frac{1}{2}}}=-\phi'(0), \tag{16}$$

$$\frac{1}{2}C_{fx}Re_x^{1/2}=f''(0). \tag{17}$$

3. Numerical Methodology

The numerical simulations of problem are performed by using shooting algorithm. The motivations for implementation shooting method are due to higher accuracy. The numerical flow chart is presented in Fig. 2. The conver-

sion of problem is based on following assumptions:

$$f = l_1, \tag{18}$$

$$f' = l'_1 = l_2, \tag{19}$$

$$f'' = l'_2 = l''_1 = l_3, \tag{20}$$

$$f''' = l'_3 = l''_2 = l_4, \tag{21}$$

$$\theta = l_5, \tag{22}$$

$$\theta' = l'_5 = l_6. \tag{23}$$

$$\emptyset = l_7. \tag{24}$$

$$\emptyset' = l'_7 = l_8. \tag{25}$$

$$l'_1 = l_2, \qquad l_1(0) = 0, \tag{26}$$

$$l'_2 = l_3, \qquad l_2(0) = 1, \tag{27}$$

$$l'_3 = l_4, \qquad l_3(0) = e_1 \tag{28}$$

$$l'_4 = \frac{1}{l_1}\Big[2l_2l_4 + l_3^2 + \frac{1}{(1+2\gamma\eta)\beta}\{(1+2\gamma\eta)l_4 + 2l_3\gamma + l_1l_3 - l_2^2 + k_1l_2 + 4\gamma\beta(l_2l_3 - l_1l_4) - Ha^2l_2 + Grl_5Cos(\alpha) + Gcl_7Cos(\alpha)\}\Big], \quad l_4(0) = e_2, \tag{29}$$

$$l'_5 = l_6, \qquad l_5(0) = e_3, \tag{30}$$

$$l'_6 = -\left(\frac{1}{\left(1+\epsilon l_5+\frac{4}{3}R\right)(1+2\gamma\eta)}\right)\Big[2\gamma l_5\left(1+\frac{4}{3}R\right) + (1+2\gamma\eta)l_6^2 \in +Prl_1l_6 + Du\big((1+2\gamma\eta)(ll_3)2\gamma l_8\big) - PrEc\beta\gamma l_1l_3^2 + PrEc(1+2\gamma\eta)(l_3^2 - \beta l_1l_3l_4 + \beta l_2l_3^2) + PrEcHa^2l_2^2\Big], \quad l_6(0) = -B_{i1}(1-e_3), \tag{31}$$

$$l'_7 = l_8, \qquad l_7(0) = e_4 \tag{32}$$

$$l'_8 = -\left(\frac{1}{(1+2\gamma\eta)}\right)[2\gamma l_8 + Scl_1l_8 + Sr((1+2\gamma\eta)(ll_2) + 2\gamma l_6)], \quad l_8(0) = -B_{i1}(1-e_4), \tag{33}$$

4. Validation of Results

The results are validated in Table 1 with analysis of Hayat *et al.* [13] for limiting case. A fine agreement of present results is noted with work of Hayat *et al.* [13].

5. Discussion

The aspect of various parameters is physically identified for velocity profile f', temperature profile θ and concentration field ϕ. Fig. 3(a-c) concentrates the impact of Hartmann number Ha on velocity profile f', temperature profile θ and concentration field ϕ. The control of fluid velocity is detected for enhancing values of Ha. The resistance in velocity is due to Lorentz force. However, the improved variation in thermal and concentration fields is noted. The magnetic force plays a significant role in

Table 1. Comparison of results for $f''(0)$ with analysis of Hayat *e al.* [13] when $\beta = 0$, $Ha = 0$.

γ	Hayat *et al.* [13]	Present results
0.1	1.0707	1.07075
0.0	1.0320	1.03206
0.1	1.0707	1.07073
0.12	1.0784	1.07841

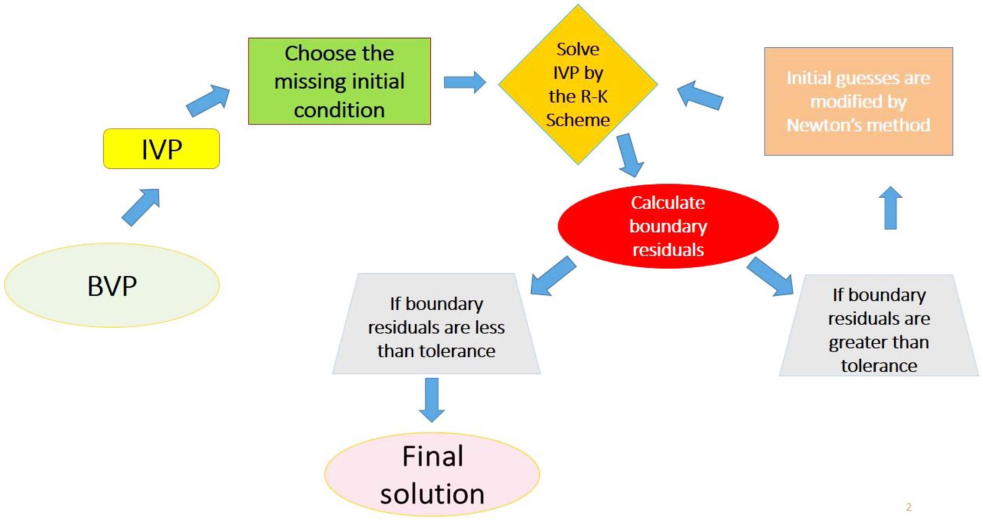

Fig. 2. (Color online) Flow chart of numerical method.

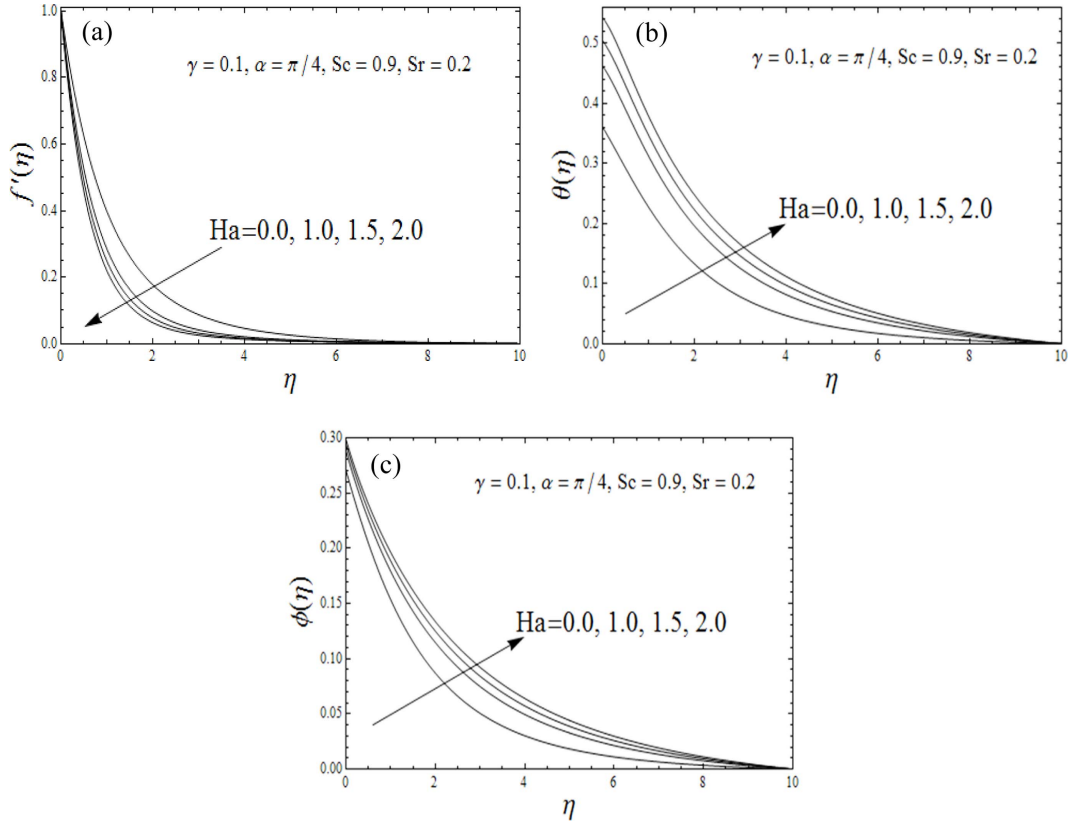

Fig. 3. (a-c) Impact of *Ha* on f', θ and ϕ.

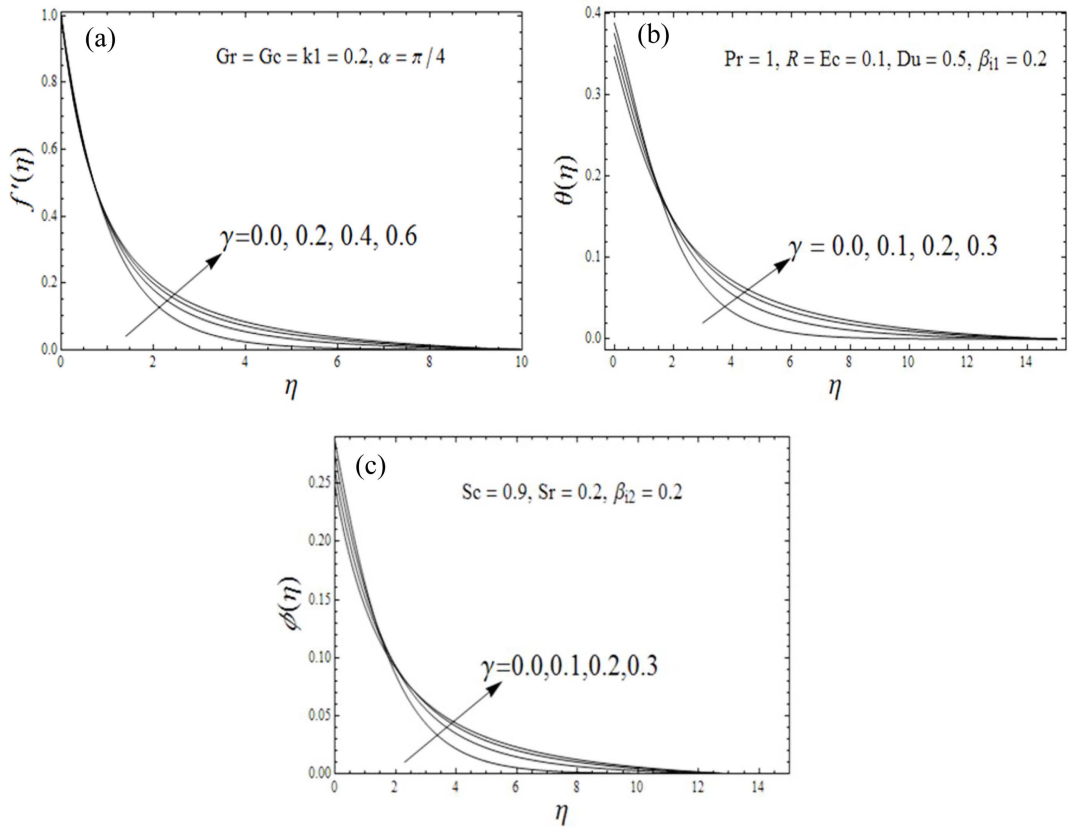

Fig. 4. (a-c) Impact of γ on f', θ and ϕ.

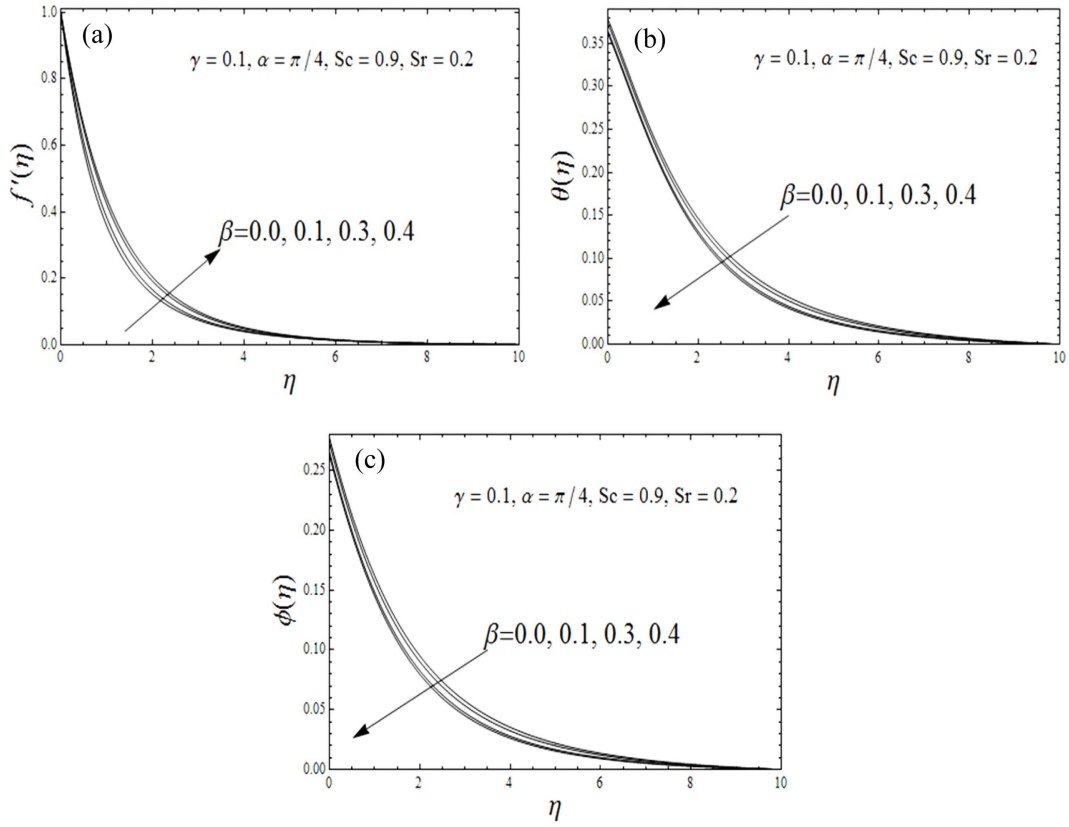

Fig. 5. (a-c) Impact of β on f', θ and ϕ.

thermal transport phenomenon. The dynamic of f' for curvature parameter γ is reported in Fig. 4(a). The enhancing deviation in velocity is subject to larger γ. However, low thermal profile is noted up to specified range and then started increases. Same observations are noted ϕ and reported in Fig. 4(b-c). In Fig. 5(a-c), the graphical predictions are claimed for viscoelastic parameter β for f', θ and ϕ. An increasing impact of β for f' is exhibited. Such observations are physically attributed to the rheology of viscoelastic fluid. In Fig. 5(b), the results are conveyed for β in order to inspect the observations for θ. A decrement in θ is visualized due to uprising in β. Fig. 5(c) expressed the aspect of ϕ due to β. The lower change in ϕ for β has been noted. Fig. 6(a-b) is prepared to report the significance of f' for thermal Grashof number Gr and concentration Grashof number Gc. An increasing claim for f' has been reported for both Gr and Gc. Physically, such increment in f' is referred to

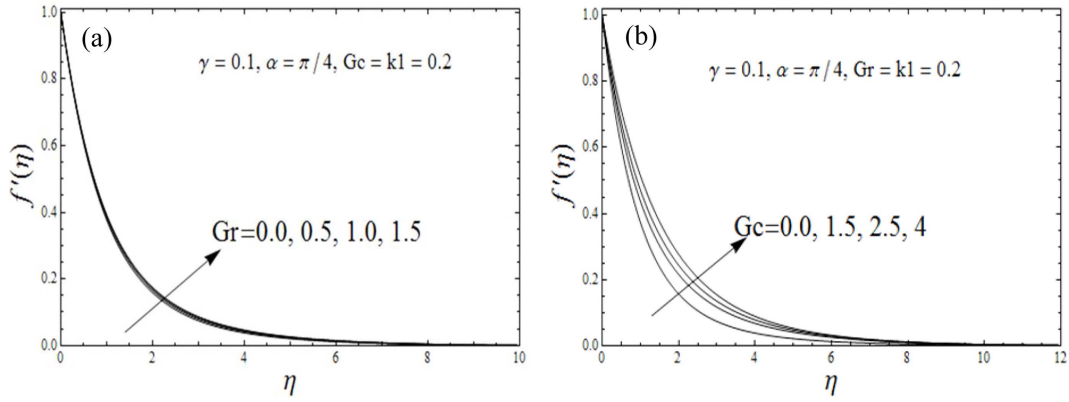

Fig. 6. (a-b) Impact of Gr and Impact of Gr on Gc on f'.

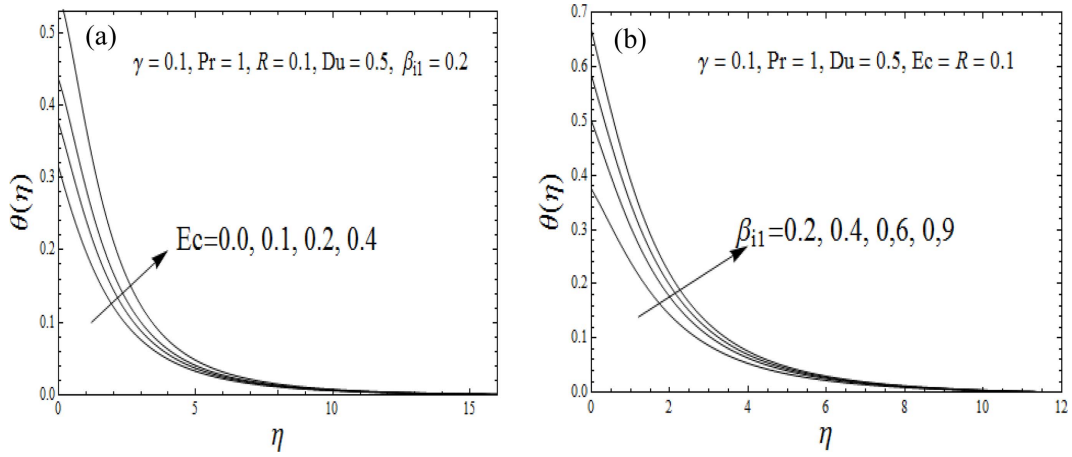

Fig. 7. (a-b) Impact of Ec and B_{i1} on θ.

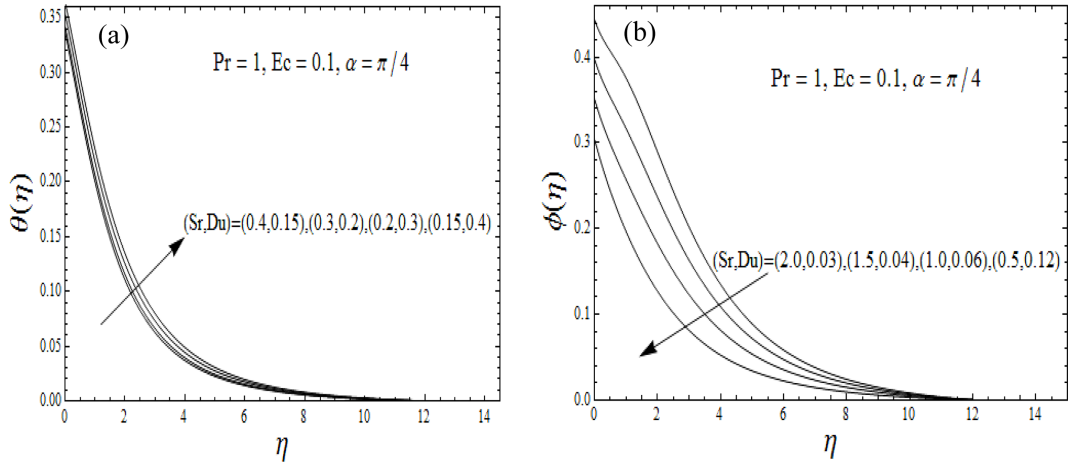

Fig. 8. (a-b) Impact of Sr and Du on θ and ϕ.

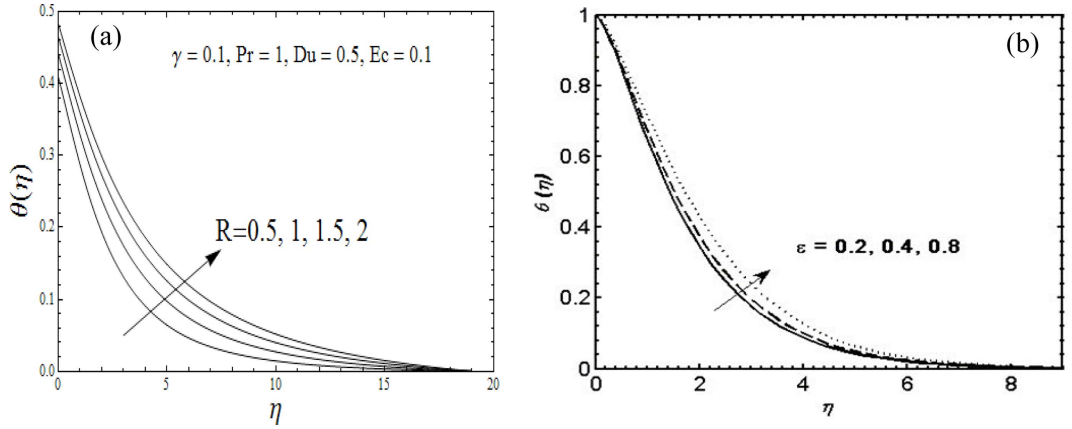

Fig. 9. (a-b) Impact of R and ε on θ.

buoyancy forces. Fig. 7(a-b) expresses the onset of Eckert number Ec and thermal Biot number B_{i1} on θ. The increment in Ec for θ is observed. Physically, larger Ec pronounced enhancing kinetic energy which increase the thermal phenomenon. Fig. 7(b) denotes the aspect of θ for B_{i1}. The temperature rate gets larger trend for B_{i1}. This increment is due to larger heat transfer coefficient.

Fig. 8(a) and (b) describes the impact of Soret number

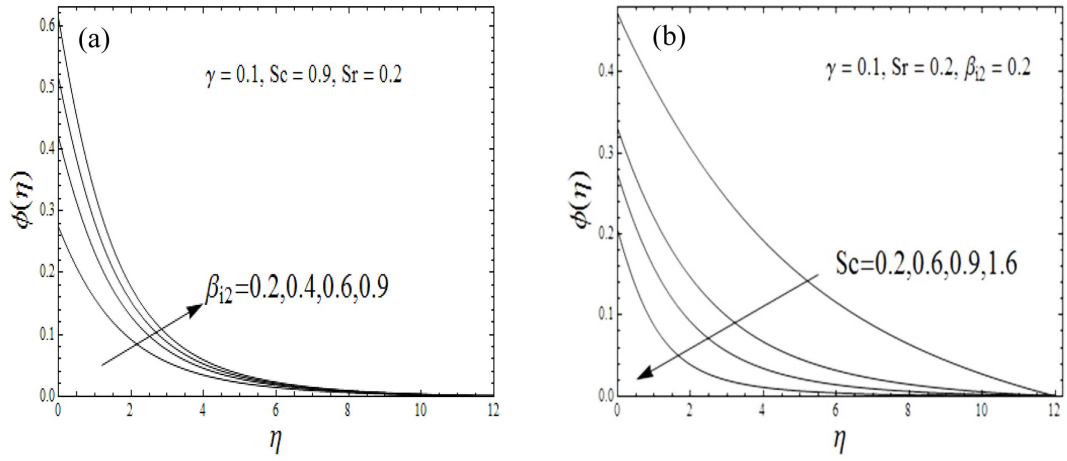

Fig. 10. (a-b) Impact of B_{i2} and Sc on ϕ.

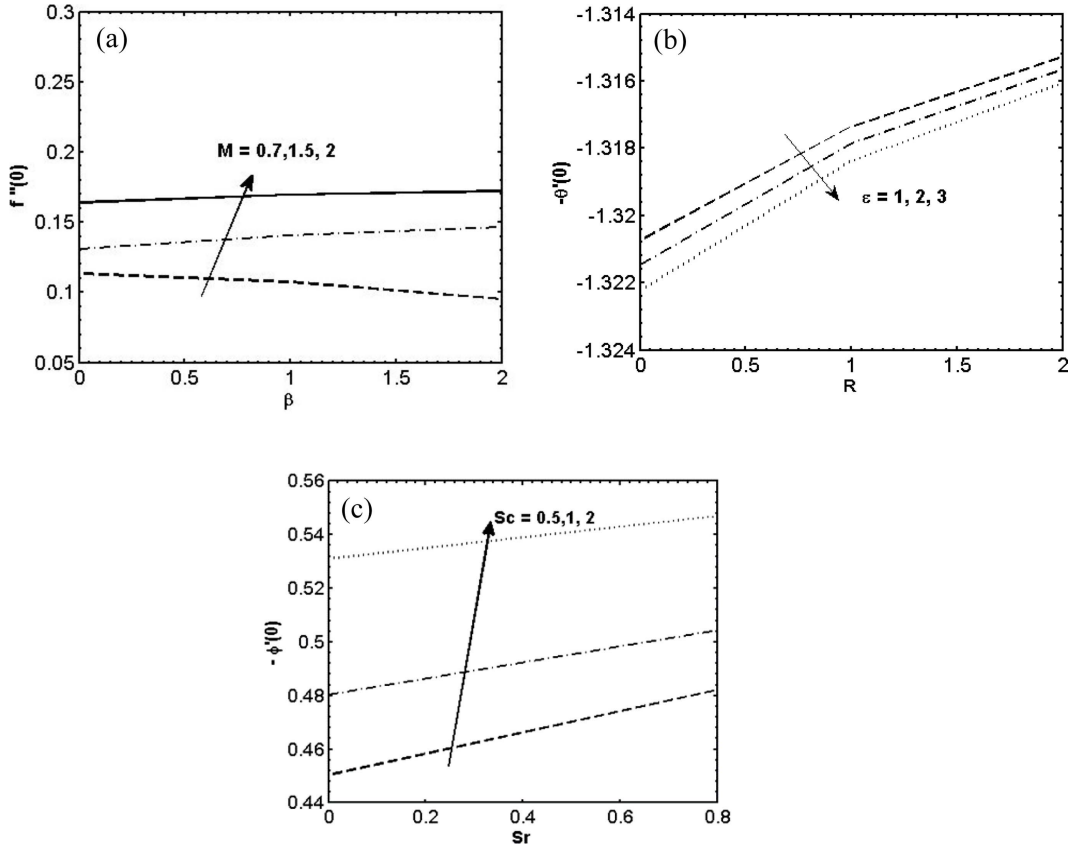

Fig. 11. (a-c) (a) Variation of $f''(0)$ with β for M, (b) variation of $-\theta'(0)$ with R for ε variation of $-\phi'(0)$ with Sr for Sc.

Sr and Dufour number Du on θ and ϕ. The enhancement in θ due to Sr and Du is exhibited. Such observations are attributed thermos-diffusion phenomenon. However, the declining rate of ϕ identified for Sr and Du. The graphical calculations of θ due to radiation factor R and variable conductivity parameter ε has been focused in Fig. 9(a-b). With increment of R, the improved profile of θ is observed (Fig. 9(a)). In radiative phenomenon, the rate of heat transfer is subject to the electromagnetic waves. Fig. 9(b) concluded the increasing influence of variable thermal conductivity for θ. Fig. 10(a) claims the onset of concentration Biot number B_{i2} on ϕ. An increment in B_{i2} results a leading impact on ϕ. From Fig. 10(b), the lower profile of ϕ is observed for Sc. Physically, larger change

in *Sc* preserve lower mass diffusivity. Fig. 11(a) presents the change in $f''(0)$ against β for *M*. The increases aspect of $f''(0)$ due to *M* is obtained. Fig. 11(b) shows that $-\theta'(0)$ gets slower profile for ε. The observations for $-\phi'(0)$ with *Sr* for *Sc* are revealed in Fig. 11(c). The increases profile of $-\phi'(0)$ has been noted for *Sc*.

6. Conclusions

The thermos-diffusion aspect of second grade fluid is observed due to inclined moving cylinder with porous space. The onset of thermal model is attributed in view of variable thermal conductivity and radiated phenomenon. Shooting numerical is used for the simulation task. Major results are:

- The velocity profile gets increasing impact due to curvature parameter and viscoelastic parameter.
- An uprise profile of velocity is noted for thermal and solutal Grashof numbers.
- Increasing thermal transport of viscoelastic fluid against Eckert number and thermal Biot number have been yield out.
- With increment to Dufour and Soret numbers, the heat transfer rate boosted.
- Lower change in concentration phenomenon is exhibited for Soret number and Dufour parameter.
- With larger variable thermal conductivity parameter, the heat transfer profile enhanced.
- The Nusselt number with viscoelastic parameter increases when Hartmann number gets varied.

Acknowledgement

Princess Nourah bint Abdulrahman University Researchers Supporting Project number (PNURSP2023R41), Princess Nourah bint Abdulrahman University, Riyadh, Saudi Arabia.

Nomenclature

(u, v) : Velocity components
g : Gravity
α : Inclined angle
α_1 : Material parameter
σ : Electric conductivity
ν : Kinematic viscosity
ρ : Fluid density
K : Permeability of porous space
$K(T)$: Temperature dependent thermal conductivity
c_p : Specific heat
T : Fluid temperature
T_∞ : Free stream temperature
C : Concentration
σ^* : Stefan Boltzmann coefficient
k^* : Mean absorption coefficient
γ : Curvature parameter
Gr : Thermal Grashof number
Gc : Solutal Grashof number
$k1$: Porosity parameter
Pr : Prandtl number
Du : Dufour number
Sr : Soret number
Ec : Eckret number
Sc : Schmidt number
B_{i1} : Thermal Biot number
R : Radiation parameter
β : Viscoelastic parameter
Ha : Hartmann

References

[1] Hashim, A. Hamid, and M. Khan, *Neural Comput. Applic* **32**, 3253 (2020).
[2] M. B. Bigdeli, M. Fasano, A. Cardellini, E. Chiavazzo, and P. Asinari, Renew. Sust. Energ. Rev. **60**, 1615 (2016).
[3] A. Tassaddiq, S. Khan, M. Bilal, T. Gul, S. Mukhtar, Z. Shah, and E. Bonyah, AIP Adv. **10**, 055317 (2020).
[4] W. Ahmed, Z. Z. Chowdhury, S. N. Kazi, M. R. Johan, N. Akram, and C. S. Oon, Int. Commun. Heat Mass Transf. **114**, 104591 (2020).
[5] A. Minaeian, M. Nili-Ahmadabadi, and M. Norouzi, Commun Nonlinear Sci Numer Simul. **83**, 105134 (2020).
[6] A. Zhu, H. Ali, M. Ishaq, M. S. Junaid, J. Raza, and M. Amjad, Energies, **15**, 5926 (2022).
[7] M. D. Shamshuddin, S. O. Salawu, H. A. Ogunseye, and F. Mabood, Int. Commun. Heat Mass Transf. **119**, 104933 (2020).
[8] A. Raza, A. Ghaffari, S. U. Khan, A. U. Haq, M. I. Khan, and M. R. Khan, Chaos, Solitons Fra. **155**, 111708 (2022).
[9] M. Ahmad, E. R. El-Zahar, K. Al-Khaled, M. Rasheed, S. U. Khan, M. Taj, M. Khan, and S. Elattar, Int. Commun. Heat Mass Transf. **135**, 106050 (2022).
[10] A. Abbasi, S. U. Khan, W. Farooq, F. M. Mughal, M. Ijaz Khan, B. C. Prasannakumara, M. Tarek El-Wakad, K. Guedri, and A. M. Galal, Ain Shams Eng. J. **14**, 101832 (2023).
[11] K. Saritha, R. Muthusami, N. Manikandan, N. Nagaprasad, and Krishnaraj Ramaswamy, Sci. Rep. **13**, 336 (2023).
[12] T. Hayat, Y. Saeed, S. Asad, and A. Alsaedi, J. Mol. Liq. **220**, 573 (2016).
[13] M. Nazeer, M. I. Khan, M. U. Rafiq, and N. B.

Khan, International Communications in Heat and Mass Transfer **119**, 104968 (2020).
[14] M. Ijaz Khan, S. Kadry, Y. M. Chu, W. A. Khan, and A. Kumar, J. Mater. Res. **9**, 10265 (2020).
[15] Y. Q. Song, M. I. Khan, S. Qayyum, R. J. P. Gowda, R. N. Kumar, B. C. Prasannakumara, Y. Elmasry, and Y. M. Chu, Mod. Phys. Lett. B **35**, 2141006 (2021).
[16] M. I. Khan, S. Qayyum, S. Kadry, W. A. Khan, and S. Z. Abbas, J. Magnetics **25**, 8 (2020).
[17] S. Farooq, M. I. Khan, A. Riahi, W. Chammam, and W. A. Khan, Comput. Meth. Prog. Bio. **192**, 105435 (2020).
[18] T. H. Zhao, M. I. Khan, and Y. M. Chu, Math. Methods Appl. Sci. https://doi.org/10.1002/mma.7310 (2021).
[19] Nan Li and Pan Gao Caihong Zhang, Sol. Energy **246**, 66 (2022).
[20] M. Yasir, M. Khan, and Z. U. Malik, Int. Commun. Heat Mass Transf. **141**, 106577 (2023).
[21] A. A. Pasha, K. Irshad, S. Algarni, T. Alqahtani, and M. Waqas, Int. Commun. Heat Mass Transf. **140**, 106519 (2023).
[22] M. Mohammadi and S. A. Gandjalikhan Nassab, Int. Commun. Heat Mass Transf. **134**, 106026 (2022).